

# Identifying and targeting resistance factors upon immune checkpoint inhibition for better combinatorial treatment strategies leading to improved outcomes

Moumita Nath<sup>1</sup>, Biswajit Das<sup>1</sup>, Juby<sup>1</sup>, Koushika R<sup>1</sup>, Kowshik Jaganathan<sup>1</sup>, Dharamidharan M<sup>1</sup>, Mouniss M<sup>1</sup>, Mohit Malhotra<sup>2</sup>, Nandini Pal Basak<sup>1</sup>, Satish Sankaran<sup>1,\*,#</sup>

<sup>1</sup>Farcast Biosciences Pvt Ltd, India, <sup>2</sup>Farcast Biosciences LLC, FL, USA.

#Presenting author, \*Corresponding author



Abstract # 822

## Background

Response to immune checkpoint inhibitor drug Nivolumab (an anti-PD1 agent), in Head and Neck Squamous Cell Carcinoma (HNSCC) is 15-20%. Using the ex-vivo TruTumor histoculture platform, we had observed that about 50% of patients did not exhibit tumor cytotoxicity despite an increased interferon gamma (IFN $\gamma$ ) release upon Nivolumab treatment [1]. In this study, we evaluated the cause for this moderate response and the possibility to improve efficacy using a combinatorial treatment strategy based on the resistance factors identified.

## Study Design

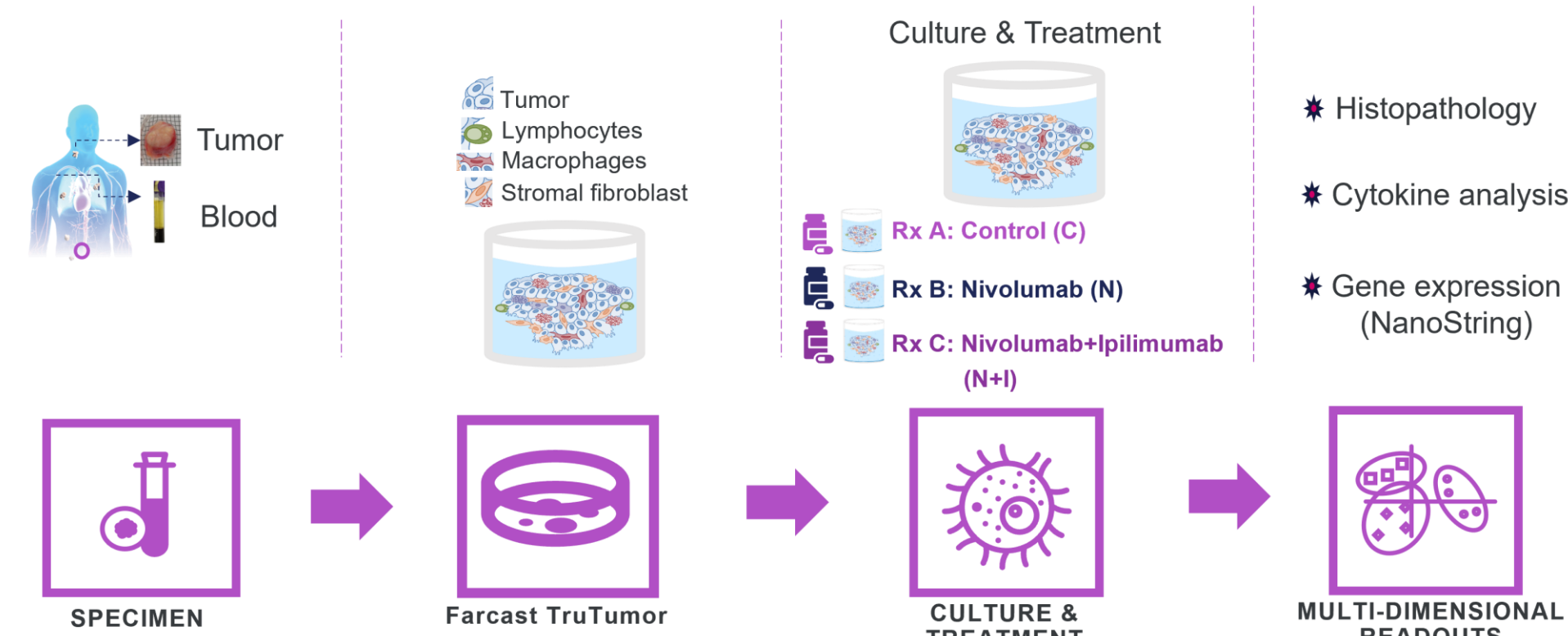


Fig. 1: Schematic representation of Farcast™ TruTumor Histoculture platform work-flow and downstream assays used for treatment response evaluation.

## Methods

**Patient tissue samples:** Fresh, surgically resected HNSCC tissue samples (n=46) were collected from consented patients along with matched blood samples.

**Histo-Culture workflow:** The tumor sample was processed to generate thin explants, without enzymatic digestion retaining the native tumor microenvironment. Tumor explants were cultured with media and autologous plasma for 72 hrs. Explants were treated with anti-PD1 (Nivolumab:132  $\mu$ g/ml) alone or in combination with Ipilimumab (90.8  $\mu$ g/ml). Media was replaced every 24 hours. Response was evaluated using cytokine analysis and NanoString based mRNA analysis.

**Cytokine Analysis:** The culture supernatants were tested at T0, T24, T48, T72 time points for the presence of cytokines (IFN-g, Granzyme-B, Perforin) using Luminex MAGPIX instrument and data was analysed using MILLIPLEX™ Analyst software.

**NanoString Analysis:** Post treatment RNA extracted arm-wise from the Tissue Micro Array (TMA) FFPE block was quantified using Tape Station. 50ng of RNA based on DV200 concentration was used for running on the nCounter PanCancer IO 360 panel. Data was normalized and analyzed using the nSolver™ Data Analysis software.

**Statistical analysis:** All data analysis and graphical representations were done using GraphPad Prism (Version 9). Mann-Whitney t-test was performed to generate p-values. p-value significance is represented as \*(p<0.05) \*\*(p<0.01) \*\*\*(p<0.001) \*\*\*\*(p<0.0001). Heat maps were generated on Morpheus (<https://software.broadinstitute.org/morpheus>).

## Patient demography

Parameters	Categories	Values (%)
Median age	≤ 57	24 (52.17%)
	> 57	22 (47.83%)
Gender	Female	28 (60.87%)
	Male	18 (39.13%)
Grade	Grade 1	33 (71.74%)
	Grade 2	12 (26.09%)
	Grade 3	1 (2.17%)
Stage	II	9 (19.57%)
	III	19 (41.3%)
	IV	18 (39.13%)
Primary/Recurrent	Primary	42 (91.3%)
	Recurrent	4 (8.7%)
Tumor Site	Alveolus	3 (6.54%)
	Buccal cavity	38 (82.61%)
	Larynx	1 (2.17%)
	Aryepiglottic fold	1 (2.17%)
	Maxilla	1 (2.17%)
	Supraglottis	1 (2.17%)
	Submandibular region	1 (2.17%)

Table 1: Demography of patient samples (n=46) used for the study.

## Nivolumab On-treatment 31-genes signature<sup>1</sup> segregates the cohort into three clusters (CL)

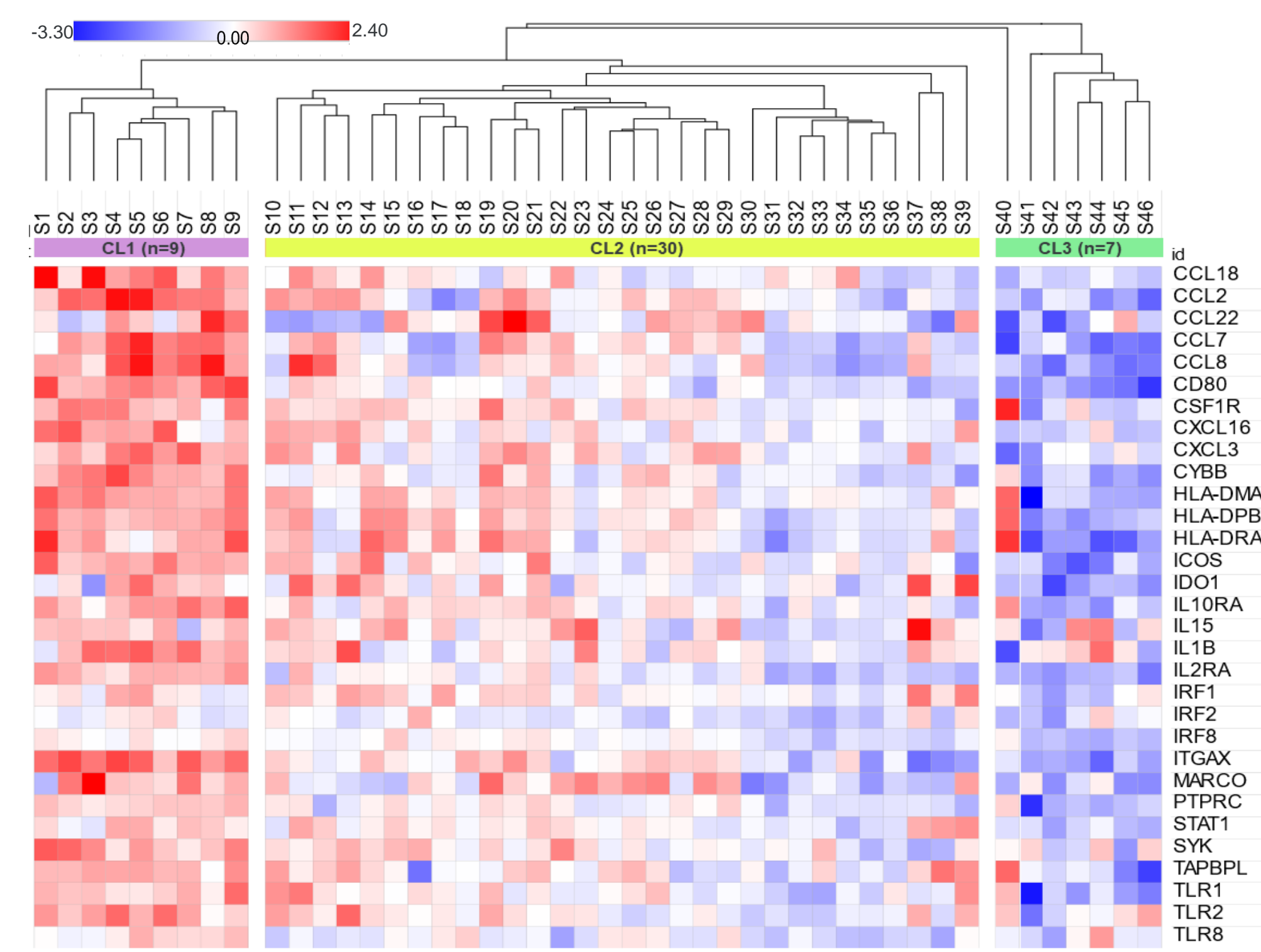


Fig. 2: Hierarchical clustering of samples post treatment with Nivolumab using the 31-gene signature. Data represents the z-score converted expression levels.

## CL1 exhibits highest immune cell activity driven tumor cytotoxicity, on treatment with Nivolumab

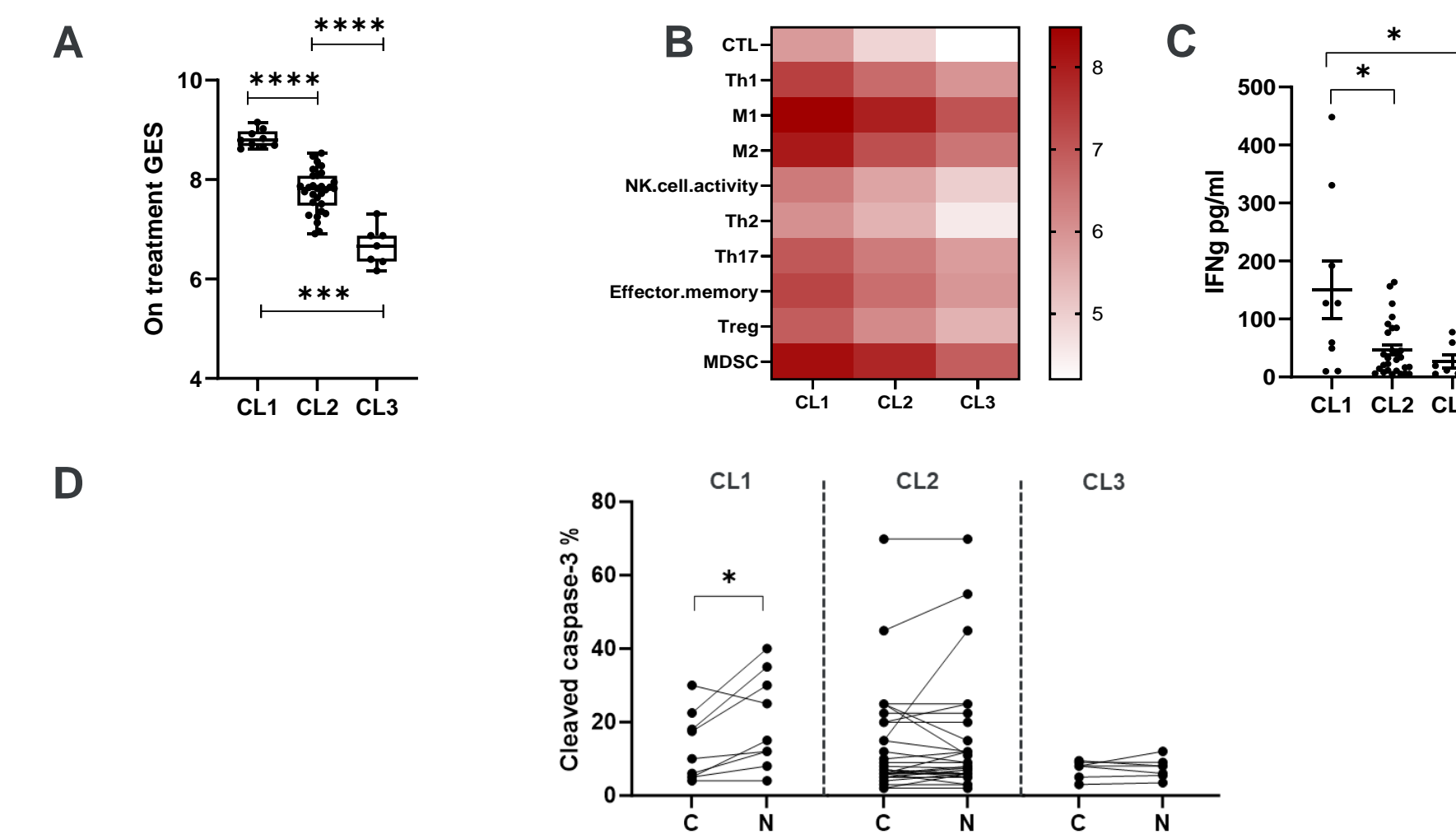


Fig. 3: (A) Box and whisker plot showing on-treatment 31-gene on-treatment GES score across the 3 clusters. (B) Heat map showing baseline immune cell population GES scores. Graph representing (C) IFN $\gamma$  secretion and (D) cleaved caspase-3 activity in control (C) and Nivolumab (N) arms in the 3 clusters.

## CL2 exhibits better immune upregulation than CL1, yet lacks treatment efficacy

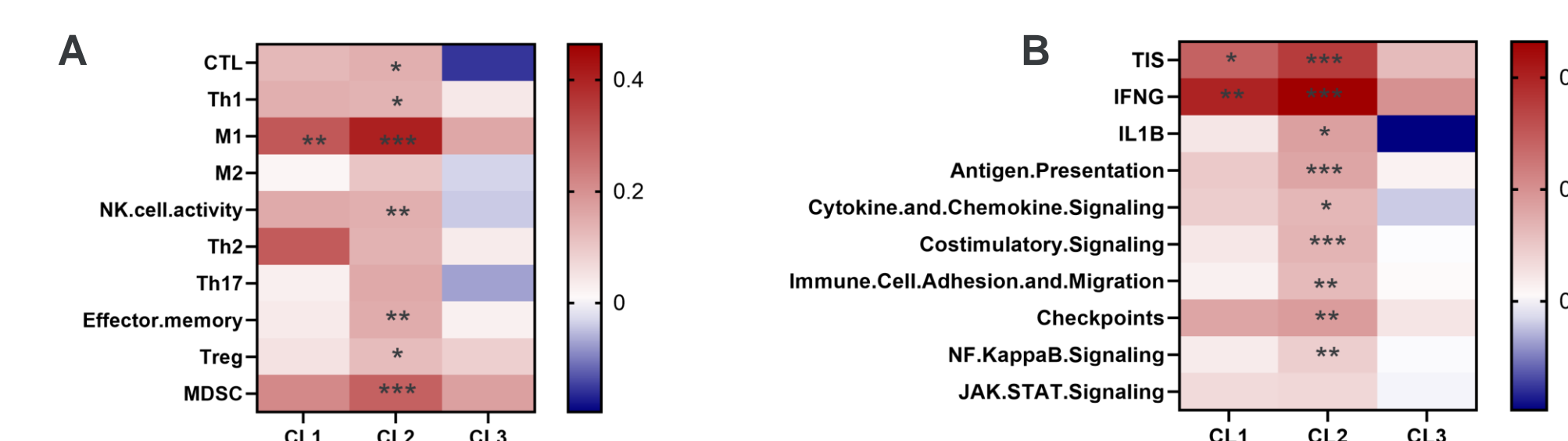


Fig. 4: Heat map showing effect of Nivolumab treatment on (A) immune cell population and (B) immune cell activity across the 3 clusters. Data represents Log<sub>2</sub> Fold change of GES and p-value significance with respect to the control arm.

## Tumor progression pathway genes are upregulated in CL2 and CL3 more than in CL1

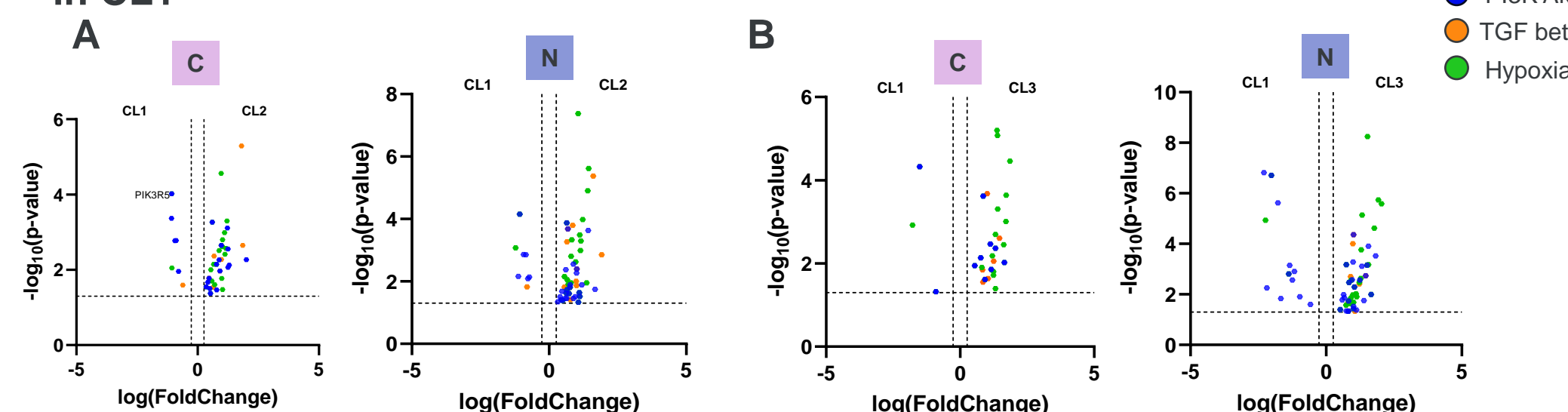


Fig. 5: Volcano plots showing comparison of CL1 with (A) CL2 and (B) CL3 for C (left) and N (right). Genes from PI3K Akt, TGF beta and hypoxia pathways that are significantly modulated are shown in different colors. Control (C) and Nivolumab (N) treated arms.

## Increase in Tregs and MDSCs on Nivolumab treatment in CL2 is reversed by combination treatment with Ipilimumab

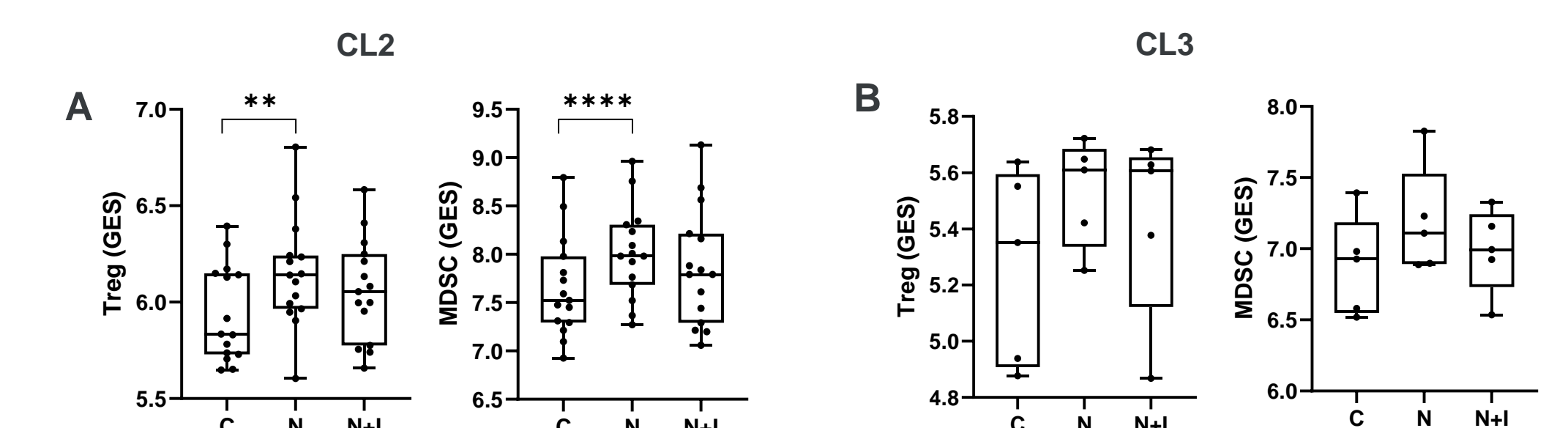


Fig. 6: Box and Whisker plot showing Treg and MDSC GES on treatment with Nivolumab (N) alone or in combination with Ipilimumab (N+I) in (A) CL2 and (B) CL3.

## Subset of CL2 exhibits improved efficacy on treatment with Ipilimumab combination, driven by NK and Effector memory cells

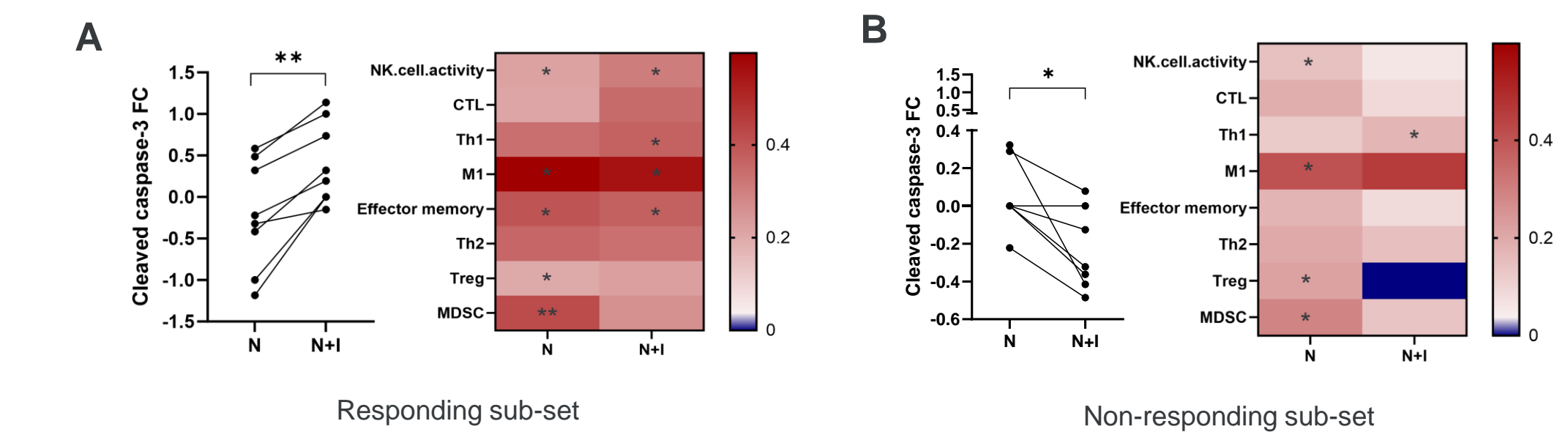


Fig. 7: CL2 segregated into (A) responding & (B) non-responding sub-sets based on improved cytotoxicity with combinatorial therapy (left). Heat maps (right) represents Log<sub>2</sub> Fold change of GES and p-value significance with respect to the control arm in the two subsets.

## CL2 non-responding sub-set is different from CL3 which displays resistance phenotype upon combinatorial treatment

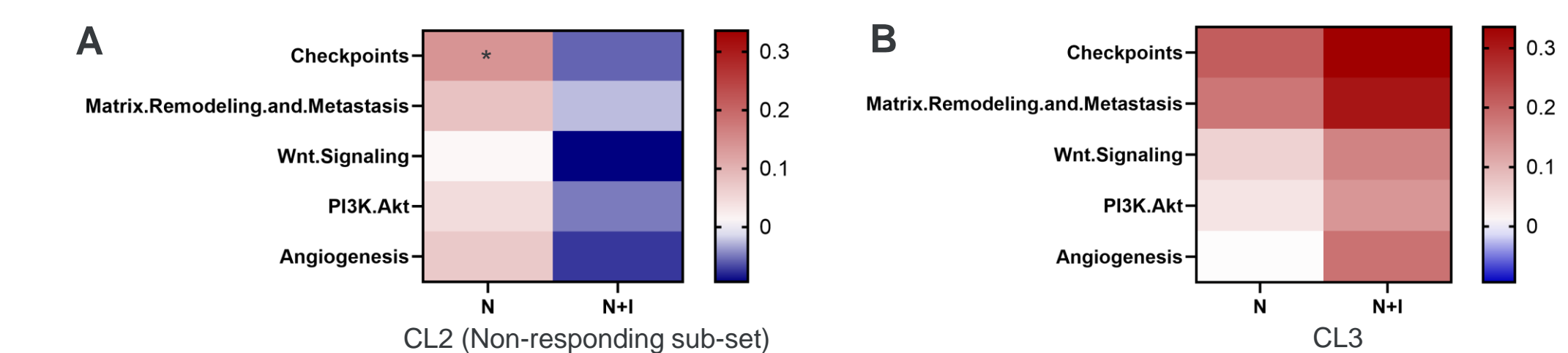


Fig. 8: Heat map showing Log<sub>2</sub> Fold change of GES and p-value significance with respect to the control arm expression for pro-tumor pathways in (A) non-responding sub-set of CL2 and (B) CL3.

## Summary

The TruTumor HNSCC histoculture platform aids in identifying combination therapies for better patient treatment outcomes.

## References

- Basak, NP, *et al.*, Nat Commun. 2024;15(1):1585.